Nonlinear Optics and Quantum Optics, Vol. 40, pp. 223–234
Reprints available directly from the publisher
Photocopying permitted by license only

Enhanced Optical Limiting Performance through Nonlinear Scattering in Nanoparticles of CdS, co-doped Ag-Cu, and BSO

P. PREM KIRAN[1,*], S. VENUGOPAL RAO[1], M. FERRARI[2], B. M. KRISHNA[3], H. SEKHAR[3], SHADAK ALEE[3] AND D. NARAYANA RAO[3,†]

[1]*ACRHEM, University of Hyderabad, Hyderabad – 500 046, India*
[*]*E-mail: premsp@uohyd.ernet.in*
[2]*CNR-IFN, CSMFO Laboratory, via alla Cascata 56/c, Povo, 38050, Trento, Italy*
[3]*School of Physics, University of Hyderabad, Hyderabad – 500 046, India*
[†]*E-mail: dnrsp@uohyd.ernet.in*

Received: June 27, 2009. Accepted: November 7, 2009.

Nanoparticles have been attracting wide interest due to their potential applications in the field of nanophotonics and optoelectronics. Most of the nanoparticles exhibit interesting nonlinear optical properties and are being used for optical limiting purposes due to absorptive nonlinearities such as, two/multi-photon absorption (TPA/MPA), excited state/Free-carrier absorption (ESA/FCA) processes etc. Though the absorptive processes often provide low limiting thresholds, most of the materials have low damage threshold limiting their applications for optical limiting studies. We present our efforts on enhancing the damage threshold through nonlinear scattering so that these materials can be used efficiently even at high input fluences. Our efforts to achieve this goal have been through the preparation and nonlinear optical characterization of metal nanoclusters, semiconductor nanoparticles, and ferroelectric nanocrystals dispersed in different media. Herein nonlinear scattering results from Ag-Cu co-doped nanoclusters in Sol-Gel films, CdS nanoparticles dispersed in dimethylformamide (DMF) and BSO nanocrystals dispersed in PMMA are presented.

Keywords: Optical limiting, nanoparticles, nonlinear scattering, nonlinear absorption.

INTRODUCTION

An ideal optical limiter, by definition, is a device that exhibits a linear transmittance below a threshold and clamps the output to a constant above it, thus

providing safety to sensors and the eyes. A wide range of materials with strong nonlinear optical properties contributing to optical limiting have been investigated [1–3]. Most of the materials, studied for optical limiting, use either of the absorptive nonlinearities or a combination of two or more processes, such as two-photon absorption (2PA), excited state absorption, free-carrier absorption [3–7]. Variety of metal nanoclusters [8–11], metal alloy nanoclusters [12], semiconductor nanoparticles [13–18], organic nanoclusters [19], in different matrices were investigated for their nonlinear optical properties. In most metal nanoclusters the effect of surface plasmon resonance was studied, while in most of semi-conducting nanoparticles nonlinear absorption (NLA) phenomena like two-photon absorption (2PA), three-photon absorption (3PA) were studied extensively [8–12]. Very few studies focused on the nonlinear scattering (NLS) phenomenon, influential at higher input fluences [11, 16, 17].

Nonlinear scattering (NLS) is a laser-induced and intensity dependent scattering. This can be observed in two different cases. In the first case, the limiting medium is a system of linear or nonlinear absorbing particles randomly distributed in a transparent host material. For a weak input light beam the temperature and refractive index changes due to the particles' absorption in the system are negligible, whereas for strong laser beam, the absorption-induced temperature change of the particles is significant and each particle forms an individual heating center. As a result of this local heating effect, the medium becomes highly inhomogeneous and considerable portions of the energy will spread out into a wider spatial region and portion of light passed through the aperture will be limited [20–22]. In the second case, the medium is a mixed system composed of two microscopic components that have similar static refractive index but are in a different phase states, e.g. one in liquid state and other is solid. If one component is transparent and the other absorbs the incident laser beam, as a result of selective opto-heating process, the whole system becomes inhomogeneous in the boundary between the two components [23–25]. NLS is a well-known phenomenon leading to optical limiting in colloidal suspensions of silica particles [26, 27], carbon particle suspensions [28,29], fullerenes [30–32], and nanoparticles [33].

In this article, we present our efforts on the NLS studies from nanoparticles dispersed in different media for optical limiting. Three different classes of nanoparticles were characterized for NLS: (a) Co-doped metal nanoclusters of sizes 10–50 nm dispersed in silica glass matrix, (b) Semiconducting CdS nanocrystals of 4.5 nm dispersed in DMF, (c) BSO nanocrystals of 62 ± 3 nm dispersed in PMMA.

EXPERIMENTAL DETAILS

Nonlinear absorption (NLA) studies were carried out using the standard open aperture Z-scan technique [34]. In a typical Z-scan experiment, a laser beam

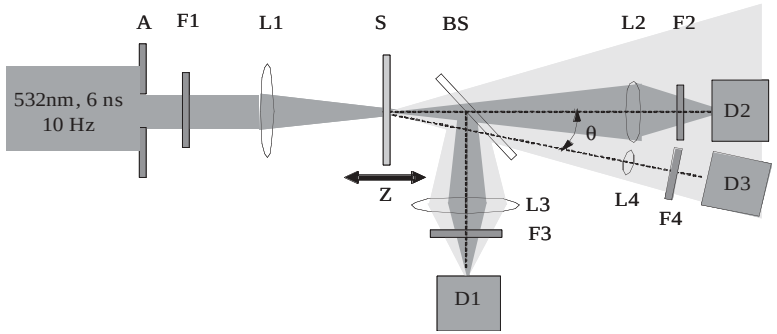

FIGURE 1
Schematic of the Z scan set up for recording the nonlinear absorption and scattering. A – aperture, S – sample, F1, F2, F3, F4 – Neutral Density Filters, D1, D2, D3 – Detectors, BS – Beam splitter, L1, L2, L3, L4 – lens.

with a transverse Gaussian profile is focused using a converging lens. The sample is then translated along the propagation direction of the focused beam. At the focal point, the sample experiences maximum pump intensity, which gradually decreases away from the focus. For simultaneous measurement of NLA and NLS standard open-aperture Z-scan is slightly modified as shown in Fig. 1. A $f/24$ focusing geometry was used for focusing the incident laser on to the sample in the present studies. A frequency doubled Nd:YAG laser (Spectra-Physics, INDI 40, 532 nm, 6 ns, 10 Hz) was used as the excitation source. Apertures were introduced in the path for beam shaping and calibrated neutral density filters were used to vary the laser intensity. The thickness of the sample was chosen to be much smaller than the Rayleigh range of the focused beam ($\sim$3 mm). The values of beam waist at focus were $\sim$20–30 μm with corresponding peak intensities in the range $\sim 10^8 - 10^9$ Wcm^{-2}. A 50–50 beam splitter introduced immediately after the sample collected the transmitted light including scattered light. This reflected beam was focused onto detector 1 by using a large area lens. Detector 1, therefore, detects only the losses due to linear and nonlinear absorption of the sample. The other half of the transmitted beam after the beam splitter was collected with a small area lens at far field to reduce the scattered light falling on detector 2. Hence, detector 2 accounted for the absorptive as well as scattering losses. The sample and beam splitter were mounted on a translation stage and detector 1 along with the collection lens L3. Detector 1 provided the "whole transmitted light" due to the nonlinear absorption alone. Detector 2, kept at the far field, recorded the transmitted beam minus the scattered beam due to both nonlinear absorption and the nonlinear scattering losses. The scattering at different forward scattering angles 'θ' with beam propagation direction was collected using detector 3. The data were recorded by scanning the sample across the focus and the transmitted beam was focused onto the photodiode (FND-100) with a lens. A boxcar averager

(model SR250) was used for signal averaging, the output of which was fed to a computer with an analog-to-digital converter (ADC) card. The sample was translated along the beam propagation direction using a computer controlled stepper motor.

RESULTS AND DISCUSSION

Three different classes of nanoparticles were investigated to establish the contribution of nonlinear scattering to the optical limiting phenomenon. The first was co-doped Ag-Cu metal nanoclusters embedded in a silica matrix; the second was semiconductor CdS quantum dots dispersed in DMF and the third being ferroelectric BSO nanoparticles dispersed in polymer film.

(A) Ag-Cu co-doped metal nanoclusters in sol-gel films

Ag-Cu co-doped metal nanoclusters were embedded in SiO_2 matrix by sol-gel technique. All the films exhibited a homogenous distribution of clusters throughout and the Cu/Ag atomic ratios were intact. The thickness of the films was 150 ± 10 nm with size of the nanoclusters varying from 10–50 nm depending on the ratio of concentration of Cu to Ag. The details of synthesis and properties of the films used in this study were reported elsewhere [35]. The on-axis transmittance data collected by detector 2 and the NLS data collected by detector 3 placed at an angle of 3.3 are shown in Fig. 2. Processes like inter-band transmission, plasmon absorption, and free-carrier absorption, are the major contributors to the observed NLA for these films,[11] leading to optical limiting. Though a weak scattering is observed up to a fluence of 10 Jcm^{-2}, a

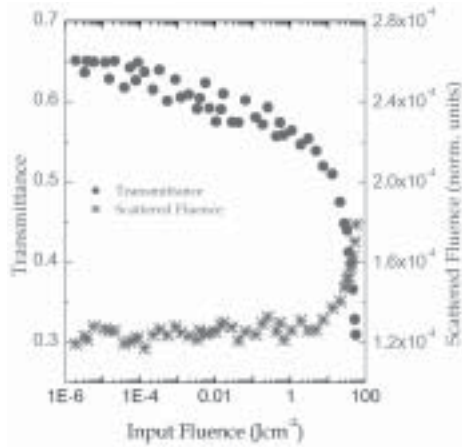

FIGURE 2
On-axis nonlinear transmittance and scattering collected at an angle of 3.3° from the beam axis for 1Ag3Cu:SiO_2 film.

dominant NLS is observed at input energies >10 Jcm^{-2} that can be seen in the far-field. Albeit the observed nonlinear scattered fluence was <500 μJcm^{-2}, contribution of NLS to the optical limiting was significant at higher input fluencies. Though the scattered fluence is small compared to the input fluence it was considerable since the films were only 150 nm thick. We believe that NLS can be increased significantly by increasing the film thickness.

(B) CdS nanoparticles dispersed in dimethylformamide (DMF)

Semiconductor CdS nanocrystals of 4.5 nm dispersed in dimethylformamide (DMF) were the second class of nanomaterials studied for the NLS properties. These nanocrystals were synthesized following the procedure suggested by Vossmeyer *et al.* [36] using thioglycerol as capping agent. The optical limiting and the scattering data recorded by placing the detectors at three positions, as explained in the experimental section are shown in Fig. 3. The CdS nanocrystals exhibited strong NLA behavior at all intensities. At peak fluences >0.6 Jcm^{-2} we observed nonlinear scattering along with strong NLA. This is evident through an enhanced depletion in the transmitted beam intensity collected with detector 2, which is reflected in the transmittance curve illustrated in Fig. 3. The scattered fluence of the CdS nanocrystals in the forward direction collected at 5° with beam propagation direction using detector 3 is shown in Fig. 3. The scattered fluence increased with increasing input fluence and is almost comparable to the losses by NLA at higher intensities. It is observed that the NLS is conical in nature with the intensity decreasing away from the center.

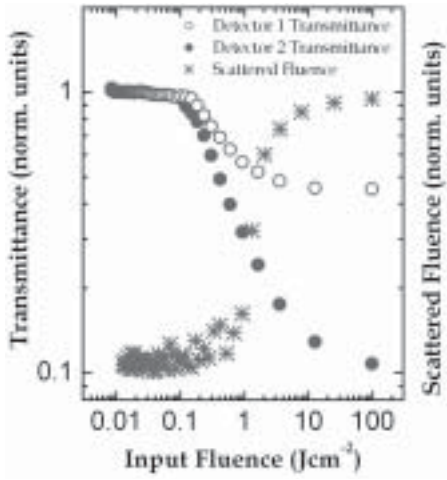

FIGURE 3
On-axis nonlinear transmittance and scattering collected at an angle of 5° from the beam axis for CdS dispersed in DMF.

Dependence of NLS on concentration of the scattering media (CdS nanocrystals) was also studied. NLS increased with increasing concentration of the CdS nanocrystals initially and then decreased. This behavior can be explained by considering the extent of non-uniform heating of the sample at the focus induced due to the 2PA of CdS nanocrystals present in the focal volume. This non-uniform heating corresponds to the change in the effective refractive index difference between (Δn_{eff}) the two components of the medium. At lower concentration the nanocrystals are far apart from each other resulting in uniform heating. As the concentration of CdS increases, there is corresponding increase in the non-uniform heating until it reaches a maximum. However, with further increase in the concentration the CdS nanocrystals move closer to each other, leading to more uniform heating of the CdS nanocrystals, and the solvent reduces the variation in refractive index due to the thermal contribution in scattering. Incidentally, the limiting threshold of the CdS nanocrystals had decreased from 1.4 Jcm^{-2} to 0.4 Jcm^{-2} with increase of concentration from 8.65×10^{-3} M/L to 10.4×10^{-2} M/L.

The observed scattering behavior was quite interesting in the sense that no scattering was observed below 0.6 Jcm^{-2} and at higher fluencies the scattering losses help achieve better limiting thresholds. Thus, CdS nanocrystals serve as good scatterer at high fluencies, without being damaged due to nonlinear absorption alone. It is apparent that at higher fluencies the losses due to nonlinear scattering is significantly large, thereby enhancing the optical limiting by reducing the limiting threshold. Quite interestingly, at higher fluencies (>6.0 J/cm^2), the forward conical scattering appeared as circular optical fringes in the transverse plane to the beam propagation direction at a far field. Similar formation of optical fringes were reported [37], when an intense laser beam passes through nanocrystallites as the refractive index of the material can be altered by the intensity of the laser beam.

(C) BSO nanocrystals dispersed in PMMA

The BSO ($Bi_{12}SiO_{20}$) nanocrystals were prepared by chemical solution decomposition (CSD) method using bismuth nitrite pentahydrite and tetra ethylorthosilicate as the starting precursors. The obtained sol was calcined followed by grinding. The powders were calcined after thorough grinding at 650 and 700°C to obtain the nanoparticles that were dispersed in PMMA. The characterization of BSO nanocrystals was carried out using different techniques such as UV-Vis absorption spectroscopy, X-Ray Diffraction (XRD) and Scanning Electron Microscopy (SEM). The absorption spectrum had a peak at $\sim$270 nm, indicating that the band gap of the BSO nanocrystals is $\sim$4.6 eV, while the band gap of the BSO single crystals is $\sim$3.25 eV [38–40]. Size of the nanocrystals estimated from width of the XRD peaks were 62 ± 3 nm. These nanocrystals were dispersed in different solutions for further characterization. Scanning Electron Microscopy (SEM) images revealed agglomeration of the particles forming clusters of 120–500 nm. Of the various solutions and

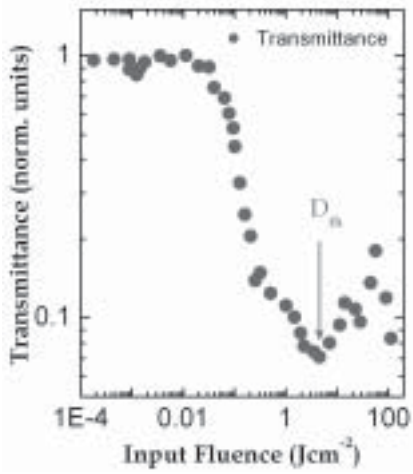

FIGURE 4
Optical limiting curve for BSO nanocrystals dispersed in PMMA. Arrow represents the damage threshold of the film $\sim$4 Jcm^{-2}.

dispersive matrices used, PMMA proved to be a better dispersive media giving relatively smaller size agglomerates. Optical limiting properties of the BSO nanocrystals dispersed in PMMA were studied.

The transmittance of BSO nanocrystals dispersed in PMMA is shown in Fig. 4. BSO nanoparticles demonstrated a good optical limiting response with a limiting threshold of $\sim$0.1 Jcm^{-2}. A dominant NLS was observed for energies $>$0.3 Jcm^{-2} and the film damaged for fluences $>$4 Jcm^{-2}. Figure 5 shows the far-field scattering distribution in the transmitted light through the film containing BSO nanocrystals. As the incident 532 nm photon energy is 2.33 eV, and the band gap of BSO nanoparticles being 4.6 eV corresponding to the absorption peak at 270 nm, 2PA is the most plausible absorptive mechanism leading to the observed optical limiting behavior. Of the various mechanisms, TPA and NLS are observed to be the major contributors leading to the optical limiting behavior.

The observed NLS in the nanomaterials were accounted by considering the difference in the effective linear and nonlinear refractive indices of both the nanoparticles and the dispersing media. As the nanoparticles showed strong nonlinear absorption, the nonlinear refractive index had a strong thermal contribution at higher fluences that increases with increasing fluence, due to the thermalization of the nanoparticles [41]. Resonant excitation with longer pulses is known to result in thermally induced transient refractive index changes, in turn depending on the thermo-optic co-efficient, the input fluence and the medium density [34].

$$\Delta n_{th} = n_{2eff} = (dn/dt)\ (F_0\alpha/2\rho_0 C_p);$$

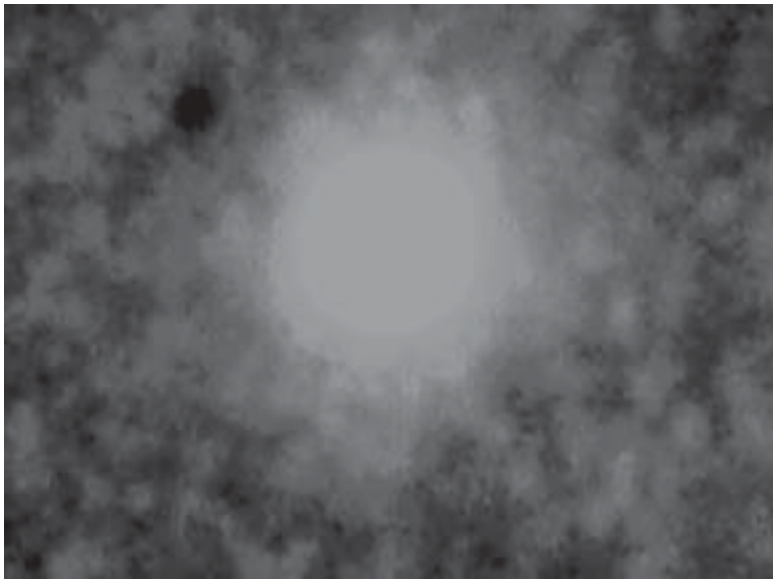

FIGURE 5
Snapshot of the transmitted beam showing the distribution of the scattering in the transmitted light through the BSO nanocrystals dispersed in PMMA film.

where dn/dt is the thermo-optic coefficient, F_0 is the light fluence, C_p is the specific heat of the nanoparticles, the medium density, 1/2 comes from the fluence averaging, and α is the nonlinear absorption coefficient of the nanoparticles.

Different mechanisms were reported leading to nonlinear scattering in variety of materials [20–33]. In a medium consisting of two components at low energy, the medium is rendered homogenous by a good refractive index matching between the two components, whereas at high energy, the intense laser light propagating through the medium makes it a heterogeneous scattering medium because of the photo-induced refractive index mismatch between the two components. In the case of nanoparticles, nonlinear scattering phenomenon is proposed to be due to induced pseudo-absorbance to the vaporization or fragmentation of the metal nanoparticles inducing a large light-scattering center around the initial particles. Such vaporization or fragmentation induced by a thermal effect has been reported earlier [26, 27, 42–44]. The energy concentrated in each particle and available to form the scattering centers is more in the nanoclusters of larger size, and size of the induced scattering centers increase with time to reach a maximum, leading to more nonlinear scattering. In case of nanoclusters suspended in solutions, at high fluences the scattering centers produces more numerous fragments confined in the same scattering center. This increases the probability of recombination with the solvent and a more

efficient cooling of the scattering centers. Such effects can be efficient in case of nanoclusters in solution state, where as in thin films such a process can lead to an irreversible damage, which was observed at higher fluences. We have observed surface damage at the fluence near 75 Jcm^{-2} where the transmission reduced drastically and the films underwent irreversible damage. Observed scattering was due to the metal nanoclusters and not due to the damage of the film, as sol-gel films are well known to remain stable up to the very high fluences, as high as 300 Jcm^{-2} in the nanosecond regime [45].

In the case of the nanoparticles in solution state, NLS is very high compared to that from films even at lower input fluences. Although nanoclusters dispersed in solution have an advantage of showing NLS comparable to NLA at lower input fluences, they suffer from low damage threshold. While the films exhibit NLS only at higher input fluences they possess higher damage threshold. As the preparation of thick films containing uniformly dispersed nanoparticles is a challenge in itself, nanoparticles in solution state would be ideal candidates for NLS purposes at lower input fluences. Nanoclusters dispersed in viscous solutions or polymer solutions may offer better NLS and provide advantage offered by both solution state and films.

CONCLUSIONS

To summarize, contribution of nonlinear scattering (NLS) from three different classes of nanoparticles dispersed in different media to the optical limiting is presented. Dependence of NLS on the input fluence, difference of refractive indices of the two components, concentration of scatterer is discussed. NLS has been found to enhance the damage threshold of the studied systems.

ACKNOWLEDGEMENTS

DNR and MF thank DST/ITPAR for funding. Part of the work has been done under the framework of ITPAR phase II (2008–2011) area ‘Nanophotonics’.

REFERENCES

[1] Bozio, R., Kajzar, F. *Eds. Optical Power Limiting*, Proceedings of the Second International Symposium [ISOPL 2000], 2–5 July 2000, Venice, Italy. Gordon Breach, 2000.

[2] Tutt, L. W , Boggess, T. F. A review of optical limiting mechanisms and devices using organics fullerenes, semiconductors and other materials. *Prog. Quantum Electron.* **17** (1993), 299–338.

[3] Sun, Y. P., Riggs, J. E. Organic and inorganic optical limiting materials. From fullerenes to nanoparticles. *Int. Rev. Phys. Chem.* **18** (1999), 43–90.

[4] La Torre, G. De., Vazquez, P., Agullo-Lopez, F. and Torres, T. Role of structural factors in the nonlinear optical properties of phthalocyanines and related compounds. *Chem. Rev*. **104** (2004), 3723–3750.

[5] Hanack, M., Schneider, T., Barthel, M., Shirk, J. S., Flom, S. R. and Pong, R. G. S. Indium phthalocyanines and naphthalocyanines for optical limiting. *Coord. Chem. Rev*. **219–221** (2001), 235–258.

[6] Calvete, M., Yang, G. Y. and Hanack, M. Porphyrins and phthalocyanines as materials for optical limiting. *Synth. Met*. **141** (2004), 231–243.

[7] Senge, M. O., Fazekas, M., Notaras, E. G. A., Blau, W. J., Zawadzka, M., Locos, O. B. and Ni Mhuircheartaigh, E. M. Nonlinear optical properties of porphyrins. *Advanced Materials* **19** (2007), 2737–2774.

[8] Zhang, Q. F., Li, W. M., Xue, Z. Q., Wu, J. L., Wang, S., Wang, D. L. and Gong, Q. H. Ultrafast optical Kerr effect of Ag–BaO composite thin films. *Appl. Phys. Lett*. **82** (2003), 958–960.

[9] Olivares, J, Requejo-Isidro, J., del Coso, R., de Nalda, R., Solis, J. and Afonso, C. N. Large enhancement of the third-order optical susceptibility in Cu-silica composites produced by low-energy high-current ion implantation. *J. Appl. Phys*., **90** (2001), 1064–1066.

[10] Qu, S., Song, Y., Liu, H., Wang, Y., Gao, Y., Liu, S., Zhang, X., Li, Y. and Zhu, D. A. Theoretical and experimental study on optical limiting in platinum nanoparticles. *Opt. Commun*. **203** (2002), 283.

[11] Prem Kiran, P., Shivakiran Bhakta, B. N., Narayana Rao, D. and Goutam De. Nonlinear optical properties and surface-plasmon enhanced optical limiting in Ag–Cu nanoclusters co-doped in SiO2 Sol-Gel films. *J. Appl. Phys.* **96** (2004), 6717.

[12] Philip, R., Ravindra Kumar, G., Sandhyarani, N. and Pradeep. T. Picosecond optical nonlinearity in monolayer-protected gold, silver, and gold-silver alloy nanoclusters. *Phys. Rev. B* **62** (2000), 13160.

[13] Lad, A. D., Prem Kiran, P., Ravindra Kumar, G. and Mahamuni, S. Three-photon absorption in ZnSe and ZnSe/ZnS quantum dots. *Appl. Phys. Lett.* **90** (2007), 133113 1–3.

[14] Lad, A. D., Prem Kiran, P., More, D., Ravindra Kumar, G. and Mahamuni, S. Two-photon absorption in ZnSe and ZnSe/ZnS core/shell quantum structures. *Appl. Phys. Lett*. **92** (2008), 043126 1–3.

[15] Nag, A., Akshay Kumar, Prem Kiran. P., Chakraborty, S., Ravindra Kumar, G. and Sarma, D. D. Optically bifunctional heterostructured nanocrystals. *J. Phys. Chem. C* **112** (2008), 8229–8233.

[16] Venkatram, N., Narayana Rao, D. and Akundi, M. A. Nonlinear absorption, scattering and optical limiting studies of CdS nanoparticles. *Opt. Exp*. **13** (2005), 867–872.

[17] Venkatram, N., Sai Santosh Kumar, R. and Narayana Rao, D. Nonlinear absorption and scattering properties of cadmium sulphide nanocrystals with its application as a potential optical limiter. *J. Appl. Phys.* **100** (2006), 74309 1–8.

[18] Venkatram, N., Satyavathi, R. and Narayana Rao, D. Size dependent multiphoton absorption and refraction of CdSe nanoparticles. *Opt. Exp*. **15** (2007), 12258–12263.

[19] Venugopal Rao, S., Venkatram, N., Giribabu, L. and Narayana Rao, D. Ultrafast nonlinear optical properties of alkyl-phthalocyanine nanoparticles investigated using Z-scan technique. *J. Appl. Phys.* **105** (2009), 053109 1–6.

[20] Soileau, M. J., Williams, W. E. and Van Stryland, E. W. Optical power limiter with picosecond response time. *IEEE J. Quant. Electron*. **19** (1983), 731.

[21] Tian, J.-G., Zhang, C., Zhang, G. and Li, J. Position dispersion and optical limiting resulting from thermally induced nonlinearities in Chinese tea liquid. *App. Opt*. **32** (1993), 6628.

[22] Khoo, I. C., Michael, R. R. and Finn, G. M. Self-phase modulation and optical limiting of a low-power CO_2 laser with a nematic liquid-crystal film. *Appl. Phys. Lett*. **52** (1988), 2108.

[23] Boggess, T. F., Moss, S. C., Boyd, I. W. and Smirl, A. L. Nonlinear-optical energy regulation by nonlinear refraction and absorption in silicon. *Opt. Lett*. **9** (1984), 291–293.

[24] Boggess, T. F., Smirl, A. L., Moss, S. C., Boyd, I. W. and Van Stryland, E. W. Optical limiting in GaAs. *IEEE J. Quantum Electron.* **QE-21** (1985), 488.

[25] Ji, W., Kukaswadia, A. K., Feng, Z. C. and Tang, S. H. Self-defocusing of nanosecond laser pulses in ZnTe. *J. Appl. Phys*. **75** (1994), 3340.

[26] Jourdier, V., Bourdon, P., Hache, F. and Flytazanis, C. Nonlinear light scattering in a two-component medium: optical limiting application. *Appl. Phys. B* **67** (1998), 627–632.

[27] Jourdier, V., Bourdon, P., Hache, F. and Flytazanis, C. Characterization of nonlinear scattering in colloidal suspensions of silica particles. *Appl. Phys. B* **70** (2000), 105–109.

[28] Nashold, K. M., Walter, D. P. Investigations of optical limiting mechanisms in carbon particle suspensions and fullerene solutions. *J. Opt. Soc. Am. B* **12** (1995), 1228–1237.

[29] Goedert, R., Becker, R., Clements, A. and Whittaker III, T. Time-resolved shadowgraphic imaging of the response of dilute suspensions to laser pulses, *J. Opt. Soc. Am. B* **15** (1998), 1442–1462.

[30] Maciel, G. S., Rakov, N. and de Araujo, Cid B. Enhanced optical limiting performance of a nonlinear absorber in a solution containing scattering nanoparticles. *Opt. Lett*. **27** (2000), 740–742.

[31] Mishra, S. R., Rawat, H. S., Joshi, M. P. and Mehendale, S. C. On the contribution of nonlinear scattering to optical limiting in C60 solution. *Appl. Phys. A* **63** (1996), 223–226.

[32] Mishra, S. R., Rawat, H. S., Joshi, M. P. and Mehendale, S. C. The role of non-linear scattering in optical limiting in C60 solutions. *J. Phys. B: At. Mol. Opt. Phys*. **27** (1994), L157–L163.

[33] Francois, L., Mostafavi, M., Belloni, J., Delouis, J.-F., Delaire, J. and Feneyrou, P. Optical Limitation induced by Gold Clusters. 1. Size Effect. *J. Phys. Chem. B* **104** (2000), 6133.

[34] Sheik-Bahae, M., Said, A. A., Wei, T., Hagan, D. J. and Van Stryland, E. W. Sensitive measurement of optical nonlinearities using a single beam. *IEEE J. Quantum Electron*. **26** (1990), 760.

[35] De, G., Tapfer, L., Catalano, M., Battaglin, G., Caccavale, F., Gonella, F., Mazzoldi, P. and Haglund. R. F. Jr. Formation of copper and silver nanometer dimension clusters in silica by the sol-gel process. *Appl. Phys. Lett*. **68** (1996), 3820–3822.

[36] Vossmeyer, T., Katsikas, L., Giersig, M., Popovic, I. G., Diesner, K., Chemseddine, A., Eychmuller, A. and Weller. H. (1994). CdS nanoclusters: Synthesis, characterization, size dependent oscillator strength, temperature shift of the excitonic transition energy, and reversible absorbance shift. *J. Phys. Chem*. **98** (1996), 7665.

[37] Mavi, H. S., Prusty, S., Shukla, A. K., Abbi, S. C. Nonlinear phenomenon in nanocrystallites produced by laser-induced etching of silicon. *Opt. Commun*. **226** (2003), 405.

[38] Hou, S. L., Lauer, R. B. and Aldrich, R. E. Transport processes of photoinduced carriers in $Bi_{12}SiO_{20}$. *J. Appl. Phys*. **44** (1973), 2652.

[39] Peltier, M., Micheron, F. Volume hologram recording and charge transfer process in $Bi_{12}SiO_{20}$ and $Bi_{12}GeO_{20}$. *J. Appl. Phys*. **48** (1977), 3683.

[40] Attard, A. E. Photoconductive and photorefractive effects in BSO. *Appl. Opt*. **28** (1989), 5169.

[41] Fleitz, P. A., Sutherland, R. L., Natarajan, L. V. Pottenger, T. and Fernelius. N. C. Effects of two-photon absorption on degenerate four-wave mixing in solutions of diphenyl polyenes. *Opt. Lett*. **17** (1992), 716–718.

[42] Link, S., El-Sayed, M.A. Spectral properties and relaxation dynamics of surface plasmon electronic oscillations in gold and silver nanodots and nanorods. *J. Phys. Chem. B*, **103** (1999), 8410.

[43] Takami, A., Kurita, H. and Koda, S. Laser-induced size reduction of noble metal particles. *J. Phys. Chem. B* **103** (1999), 1226.

[44] Fujiwara, H., Yanagida, S. and Kamat, P. V. Visible laser induced fusion and fragmentation of thionicotinamide-capped gold nanoparticles. *J. Phys. Chem. B* **103** (1999), 2589.

[45] Smilowitz, L., McBranch, D., Klimov, V., Grigorova, M., Weyer, B. J., Koskelo, A., Mattes, B. R., Wang, H. and Wudl. F. Fullerene doped glasses as solid state optical limiters. *Synthetic Metals* **84** (1997), 931.